2005

Calcareous Nannoplankton Response to Late Albian Oceanic Anoxic Event 1d in the western North Atlantic

David K. Watkins
University of Nebraska-Lincoln, dwatkins1@unl.edu

Matthew J. Cooper
Southampton Oceanography Centre, School of Ocean and Earth Science, Southampton, UK

Paul A. Wilson
Southampton Oceanography Centre, School of Ocean and Earth Science, Southampton, UK

Calcareous nannoplankton response to late Albian oceanic anoxic event 1d in the western North Atlantic

David K. Watkins
Department of Geosciences, University of Nebraska, Lincoln, Nebraska, USA

Matthew J. Cooper and Paul A. Wilson
Southampton Oceanography Centre, School of Ocean and Earth Science, Southampton, UK

Received 10 October 2004; revised 14 January 2005; accepted 17 February 2005; published 3 June 2005.

[1] Well-preserved nannofossil and stable isotope records from the mid-Cretaceous of Ocean Drilling Project Leg 171B (western North Atlantic) indicate cyclical, productivity-based variations in surface water characteristics, suggesting orbitally paced changes in upwelling intensity and the strength of deep mixing associated with oceanic anoxic event (OAE)1d. Paleontologic and isotopic evidence suggest that collapse of upper water column stratification associated with OAE1d was preceded by approximately 1 m.y. of progressively decreasing water column stability and increasing surface water fertility. Thirteen species went extinct during a short (ca. 200 k.y.) interval associated with OAE1d. Nine of these have morphological characters suggesting adaptation to specific depths in the photic zone. Simultaneous extinction of these depth-zoned species suggests that stratification collapse disrupted the habitat space for these specialized forms, resulting in extinction. A cyclostratigraphic model provides age estimates of several important nannofossil datums including the first appearances of *Eiffellithus turriseiffelii* (100.95 Ma) and *Corollithion kennedyi* (99.55 Ma).

Citation: Watkins, D. K., M. J. Cooper, and P. A. Wilson (2005), Calcareous nannoplankton response to late Albian oceanic anoxic event 1d in the western North Atlantic, *Paleoceanography*, *20*, PA2010, doi:10.1029/2004PA001097.

1. Introduction

[2] Oceanic anoxic events (OAEs) were geologically short-term perturbations in the global carbon cycle that resulted in the widespread burial of organic carbon-rich marine sediments, often including laminated black shales. They were agents of strong evolutionary selective pressures on plankton communities during the mid-Cretaceous [*Erbacher and Thurow*, 1997; *Leckie et al.*, 2002]. Species turnover rates of 25–50% of the total radiolarian assemblage [*Erbacher and Thurow*, 1997] and 20–30% of the planktonic foraminiferal assemblage [*Leckie et al.*, 2002] have been reported for the mid-Cretaceous OAEs. These high rates of turnover are rendered more striking by the fact that different paleoceanographic mechanisms are invoked to explain different OAEs. The giant OAEs of the mid-Cretaceous (OAE1a and OAE2) appear to have been the result of increased nutrient influx to the upper water column through intensified upwelling or deep mixing, as evidenced by marked positive carbon isotope excursions and the marine nature of the preserved organic material [*Arthur et al.*, 1987, 1990; *Bralower et al.*, 1994; *Erbacher et al.*, 1996; *Leckie et al.*, 2002]. A similar episode of enhanced fertility, coupled with a collapse of the upper water column stratification through mixing, appears to have driven organic carbon sequestration during OAE1d [*Wilson and Norris*, 2001]. Early Albian OAE1b, on the other hand, has been interpreted in a number of ways. *Erbacher et al.* [2001] interpreted OAE1b as representing an interval of increased stratification through increased surface water temperature and fresh water influx leading to reduced deepwater formation and oceanic stagnation. *Leckie et al.* [2002] proposed that OAE1b was triggered by an influx of micronutrients resulting from elevated submarine hydrothermal activity at a time when the water column was weakly stratified. *Herrle et al.* [2003b] proposed that OAE1b resulted from variable surface water productivity due to increasing monsoonal circulation coupled with reduced deepwater ventilation. These types of events would have imposed markedly different selective pressures on plankton communities.

[3] The evaluation of paleoecological evolution in nannoflora assemblages across OAE1d has been aided by beautiful calcareous nannofossil preservation in upper Albian and lower Cenomanian pelagic sedimentary sections drilled by the Ocean Drilling Program (ODP) on Leg 171B (Holes 1052E and 1050C) and from Deep Sea Drilling Project (DSDP) Hole 392A on Blake Nose in the western North Atlantic (Figure 1). Similarly, preservation of pristine, "glassy" planktonic foraminiferal calcite in these strata has allowed detailed stable isotope investigation of foraminiferal paleoecology, ontogeny, and paleoceanographic change to upper water column stratification and carbon cycling in late Albian–earliest Cenomanian time [*Norris and Wilson*, 1998; *Wilson and Norris*, 2001]. More generally, oxygen isotopes of planktonic foraminifers from Deep

0883-8305/05/2004PA001097$12.00

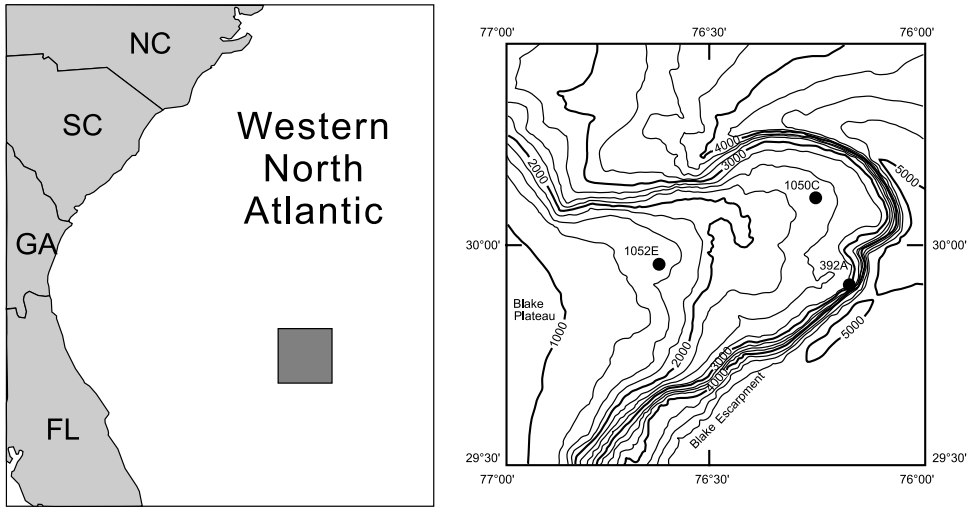

Figure 1. Location of ODP Holes 1050C and 1052E and DSDP Hole 329A on Blake Nose, western North Atlantic. (left) Regional map shows southeastern seaboard of the North America with shaded box indicating position of (right) large-scale map.

Sea Drilling Project (DSDP) Hole 392A indicate a weakly stratified upper water column, and planktonic-benthic isotopic gradients suggest a weak stratification between surface and intermediate deep waters, during the latest Aptian [*Leckie et al.*, 2002]. By the middle Albian, records indicate an overall increase in surface water temperatures and a significant increase in the surface to deep gradient [*Fassell and Bralower*, 1999; *Leckie et al.*, 2002]. Detailed records from multiple species of planktonic foraminifers from black shale intervals in ODP Hole 1052E indicate a well-stratified upper water column, characterized by very warm sea surface temperatures (SSTs exceeding 30°C [*Norris and Wilson*, 1998; *Wilson and Norris*, 2001]) during the early late Albian. Thermocline temperatures exhibited a progressive increase through the late Albian (Figure 2). Sea surface temperatures varied significantly (approximately 5°C, Figure 2), resulting in periods of strong stratification (with warm SSTs) and weak stratification (corresponding to cooler SSTs) during the late Albian [*Wilson and Norris*, 2001]. This well-stratified thermal structure collapsed abruptly during OAE1d, as evidenced by the convergence of the oxygen isotope values of thermocline and surface dwelling planktonic foraminifers [*Wilson and Norris*, 2001]. This stratification collapse was accompanied by the deposition of black shale facies and a positive carbon isotope excursion, interpreted to reflect a globally significant interval of organic carbon burial [*Wilson and Norris*, 2001]. Stratification of the water column was reestablished in the Cenomanian, and persisted through Turonian time [*Huber et al.*, 1999; *Norris et al.*, 2002; *Wilson et al.*, 2002].

[4] Here we report analyses from the thick sections of cyclically interbedded clay-rich pelagic carbonates and organic carbon-rich mudstones spanning OAE1d. These sections contain ''glassy'' planktonic foraminifers and exquisite calcareous nannofossils from Holes 1050C (nannofossil data only) and 1052E (bulk sediment stable isotope and nannofossil data) which were examined at several levels of detail to analyze the paleoenvironmental nature of the event on Blake Nose and its effects on the standing crops of calcareous nannoplankton.

2. Materials and Methods

[5] One hundred twenty eight samples from ODP Holes 1050C and 1052E were prepared as smear slides and examined to determine biostratigraphic ranges, semiquantitative species abundances, preservation, and abundance of calcareous nannofossils as a sedimentary component. A composite section was constructed using planktonic foraminiferal and calcareous nannofossil biostratigraphy. The stratigraphic section was correlated to the geochronologic timescale using a modified version of the orbital cyclostratigraphy of *Wilson and Norris* [2001]. The cyclostratigraphy was modified by changing the placement of the Albian/Cenomanian boundary to conform to the more recent planktonic foraminiferal biostratigraphy of *Bellier et al.* [2001], and by extending the cyclostratigraphy further into the Cenomanian. This age model assumes that the Albian/Cenomanian boundary is 99.6 Ma, following *Gradstein et al.* [2004].

[6] From the 128 samples, 58 were chosen to quantitatively determine the distribution of major taxa through the upper Albian and lower Cenomanian; sample selection was based on stratigraphic position and preservation. Most of these samples were chosen from the darkest lithology available from a given core interval. This practice yielded samples with the best preservation as well as providing a means to monitor the relative strength of the paleoceanographic phenomena responsible for the deposition of these organic-rich beds through the section.

[7] Precessional cycles in the upper Albian shale and clayey limestone couplets were identified by analysis of neutron porosity logs [*Wilson and Norris*, 2001]. One core section (1052E-39R-5, upper Albian) with particularly well-defined shale-limestone couplets was sampled (1 cm interval) to determine the detailed behavior of the nannofossil

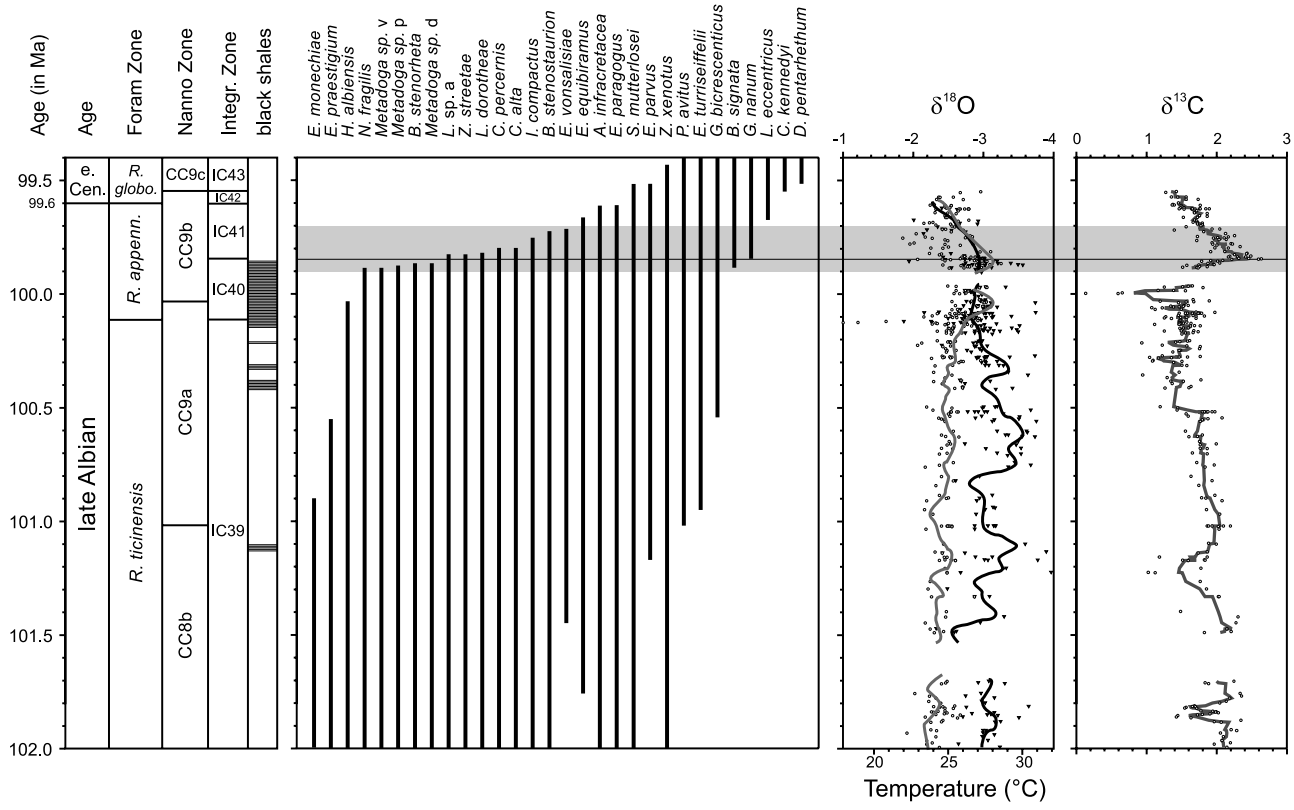

Figure 2. Biostratigraphy of selected taxa from ODP Leg 171B. Age assignments are based on *Wilson and Norris* [2001] recalibrated by setting the Albian/Cenomanian boundary at 99.6 Ma. Foraminiferal biostratigraphy is from *Bellier et al.* [2001]. The distribution of laminated black shale facies, based on data from *Norris et al.* [1998], is illustrated by horizontal shading. Nannofossil species are plotted as range-through distributions. Oxygen and carbon isotope data are from *Wilson and Norris* [2001]. Black lines indicate the five-member moving average of isotopic values from thermocline-dwelling species, while the shaded line indicates the moving average of surface-dwelling planktonic foraminifers. The interval of increased extinction (from 99.7 to 99.9 Ma) is indicated by a shaded horizontal band. The level of the maximum positive carbon values in the positive excursion is indicated by a horizontal black line.

and bulk sediment $\delta^{13}C$ records. Raw sediment from these samples was pulverized, treated with H_2O_2 to remove organics, and dried at 50°C. Carbon isotopes were determined using a Europa Geo 20-20 mass spectrometer with a CAPS preparation system. The precision of these analyses was better than 0.1‰ relative to the Vienna Pee Dee Belemnite (VPDB) standard. We do not interpret oxygen isotope data because the oxidative pretreatment technique used compromises the fidelity of these analyses.

[8] Paleontological and sedimentological counts were generated from sediment smear slides prepared using a double slurry method shown to yield reproducible data at the 99.99% confidence level (see *Watkins and Bergen* [2003] for detailed discussion). Counts were performed using a double blind protocol. Point counts were used to determine abundance of nannofossils relative to other carbonate grains. The census counts of 456 nannofossils per sample were statistically examined by correlation and principle components analyses. Indices for diversity, dominance, and fertility were calculated. Much of this computation work was performed using the PAST statistical program [*Hammer et al.*, 2001]. Data are archived at the World Data Center-A for Paleoclimatology [*Watkins et al.*, 2005].

3. Results

3.1. Biostratigraphy

[9] A total of 164 taxa were identified from the upper Albian and lower Cenomanian of Sites 1050C and 1052E. One hundred and five species (64%) range through the entire composite section. Another 27 taxa are too rare in abundance and sporadic in occurrence at Blake Nose, and are too poorly documented in the published literature, to determine confidently their stratigraphic ranges and are not considered further in this study. Thirty-two taxa (20%) have reliable first or last occurrences in this section (Figure 2). Some of these taxa are used to assign nannofossil subzones and, in combination with data from *Bellier et al.* [2001], to foraminiferal and integrated microfossil zones (Figure 2). Age assignments for these events are listed in Table 1.

[10] The stratigraphic distribution of biohorizons in this sequence is unevenly spaced. The interval from 101.3 to

Table 1. Geochronologic Age Estimate of Selected Biostratigraphic Events From Blake Nose

	Event	Age Estimate,[a] Ma	Zonation Usage
Z. xenotus	LAD	99.43	
D. pentarhethum	FAD	99.52	
E. parvus	LAD	99.52	
S. mutterlosei	LAD	99.52	
C. kennedyi	FAD	99.55	base of CC9c, IC43
R. globotruncanoides[b]	FAD	99.60	base of IC42
E. paragogus	LAD	99.61	
A. infracretaeca	LAD	99.61	
E. equibiramus	LAD	99.66	
L. eccentricum	FAD	99.68	
E. vonsalisiae	LAD	99.72	
B. stenostaurion	LAD	99.73	
I. compactus	LAD	99.75	
C. alta	LAD	99.78	
C. percernis	LAD	99.80	
L. dorotheae	LAD	99.82	
L. apocalyptica	LAD	99.82	
Z. streetiae	LAD	99.82	
G. nanum	FAD	99.85	base of IC41
B. stenorheta	LAD	99.87	
Metadoga sp. d	LAD	99.87	
Metadoga sp. p	LAD	99.88	
B. signata	FAD	99.89	
N. fragilis	LAD	99.89	
Metadoga sp. v	LAD	99.89	
H. albiensis	LAD	100.03	base of CC9b
R. appenninica[b]	LAD	100.12	base of IC40
G. bicrescenticus	FAD	100.54	
E. praestigium	LAD	100.55	
E. monechiae	LAD	100.90	
E. turriseiffelii	FAD	100.95	base of CC9, NC10
P. avitus	FAD	101.02	
E. parvus	FAD	101.17	
E. vonsalisiae	FAD	101.45	
E. equibiramus	FAD	101.76	
Base of section		102.0	

[a]Age estimate is based on the stratigraphic position of the events in Hole 1052E for events older than 99.6 Ma; those younger than 99.6 Ma are based on the stratigraphic position in Hole 1050C. The second decimal place is not a significant figure but is shown only to indicate the relative ordering of events. Note that some of these events may be local disappearances and not represent the true extinction levels (see text).

[b]Stratigraphic placement of planktonic foraminiferal events are from *Bellier et al.* [2001].

99.2 Ma is characterized by a modest net increase in the species richness (Figure 3), arising from the presence of six first appearance datums (FADs) and only three last appearance datums (LADs). This yielded an average rate of 0.45 events per 100 k.y. Much of this activity is attributable to the adaptive radiation within the genus *Eiffellithus*, as documented from this stratigraphic section by *Watkins and Bergen* [2003]. The succeeding 200 k.y., from 99.2 to 99.0 Ma, were characterized by a greatly accelerated rate of species turnover (speciation plus extinction), with an average of 7.5 events per 100 k.y. This significantly higher turnover rate is largely the result of a rapid rate of extinction, with 13 taxa having LADs. This episode resulted in a net loss of 11 species, or approximately 7% of the total richness. Subsequently (corresponding to 99.0 to 98.7 Ma in the age model), the rate of extinction decreased and, offset by the introduction of three Cenomanian taxa, resulted in a cumulative net loss of about 10 taxa (Figure 3).

3.2. Distribution of Major Taxa

[11] Examination of the count data for the 58 samples spaced throughout the section reveals that five taxa have abundances that approach or exceed 10% in any sample, and that these taxa constitute an average of about 40% of the assemblage. *Zeugrhabdotus moulladei* (this small species has often been referred to as *Zeugrhabdotus erectus* in the literature) is the most abundant species with an average abundance of about 14% and an abundance range of 5–25%. This species shows no clear trend in abundance through the section. Two of the three peaks in abundance (>∼20%) coincide with black shale deposition, while the third occurs during the interval of rapid extinction associated with OAE1d (Figure 4).

[12] The second most abundant species, *Biscutum constans*, has an average abundance of about 12% and a range of 5–23%. There was a progressive increase in abundance from values <10% between 101.2 to 102 Ma to abundances >15% from about 99.7 to 99.9 Ma. This progressive increase in abundance can be approximated by a second-order growth curve with $r = 0.78$. There was a brief decline in abundance near the Albian/Cenomanian boundary, followed by a recovery to former values. There is a weak positive correlation between *Z. moulladei* and *B. constans* ($r = 0.42$, $p = 0.001$), suggesting that the two show similar trends in abundance, but this is largely the result of correlation of outlier points.

[13] The third major species, *W. barnesiae*, is characterized by a relatively stable abundance level, averaging 7%, from about 100.5 to 102 Ma. The average abundance level decreased to an average of about 4% from 99.7 to 100.5 Ma, although peak values still exceed 10%. Its abundance significantly increases to average levels of 14% near the Albian/Cenomanian boundary (Figure 4), and these higher values are maintained into the early Cenomanian. This species has low correlations with *B. constans* ($r = -0.26$) and *Z. moulladei* ($r = -0.44$), suggesting that its distribution pattern is not wholly the result of closure with the other two major taxa.

[14] The nannoconids and braarudospheres are abundant only in the lower portion of the section, because both were involved with the rapid extinction episode associated with OAE1d. The abundance of nannoconids is quite variable from 99.9 to 102 Ma (1.8–13.4%), although there is a clear trend of decreasing maximum values with time through this interval (Figure 4). The braarudosphaeres exhibit a more striking pattern of progressive decrease before their extinction at about 99.9 Ma. This pattern of decrease can be approximated closely by an exponential decay curve with $r = 0.92$ (Figure 4).

3.3. Precessional Cycles

[15] The abundance of calcareous nannofossil relative to other carbonate grains was assessed by point count from samples in section 1052E 39R-5. Other carbonate grains consist of recognizable foraminiferal shell material (retaining the radial prismatic microstructure and shell perforations) as well as micrite of uncertain origin. Analysis indicates a relationship between the proportion of the coccoliths comprising the carbonate fraction of the sediment

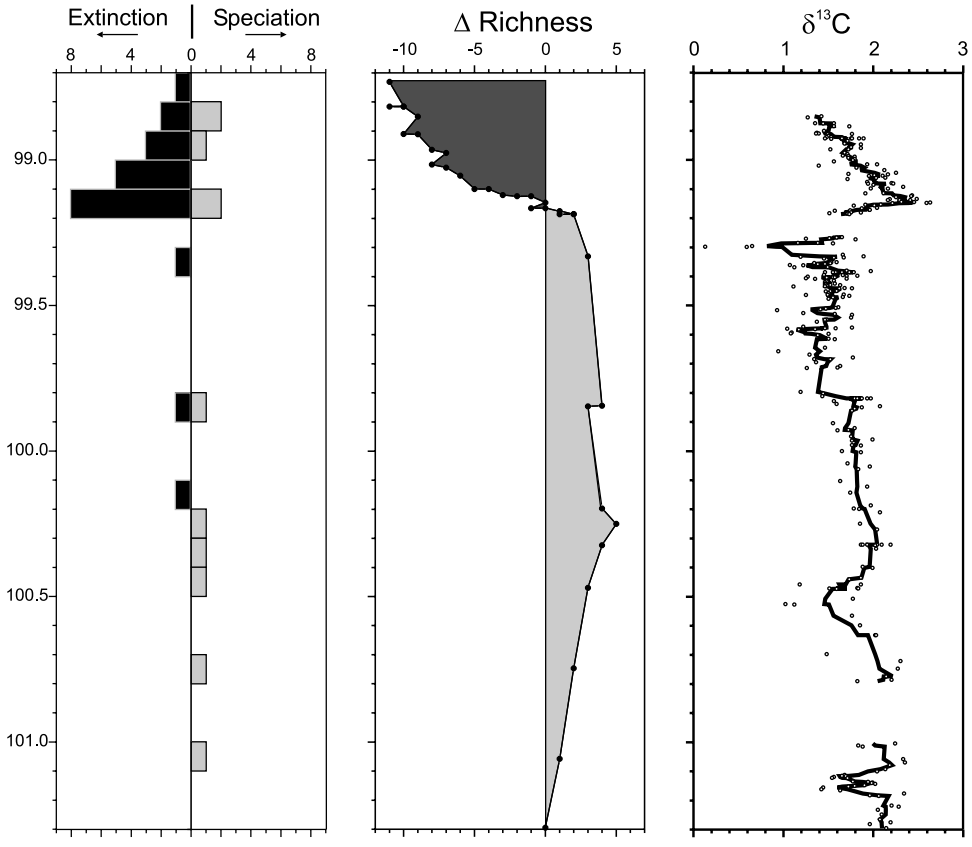

Figure 3. Evolutionary changes in species richness. Distribution of speciation and extinction events is based on stratigraphic ranges compiled in Figure 2. Cumulative changes in species richness (Δ Richness) indicate significant interval of extinction is coincident with a large positive carbon isotopic excursion.

and the carbon isotopic signal (Figure 5). The proportion of coccoliths closely mimics the bulk sediment carbonate $\delta^{13}C$ record, as indicated by a high correlation ($r = 0.85$, $n = 149$, $p = <1 \times 10^{-100}$).

[16] Sediment color, as measured by reflectance (L*), exhibits a negative correlation with $\delta^{13}C$ ($r = -0.78$). Although only 29 reflectance measurements were taken by the Leg 171B shipboard science party for this interval, the correlation between $\delta^{13}C$ and L* is still significant ($p = 6.7 \times 10^{-7}$), with darker calcareous shale characterized by higher $\delta^{13}C$ values. The correlation of L* with percentage of nannofossils is slightly higher ($r = -0.86$, $p = 2.8 \times 10^{-9}$) indicating that the carbonate in the darker clay stone is dominated by nannofossils, while the limestones are dominated by foraminiferal carbonate and micrite.

[17] We calculated Shannon Diversity index for 130 samples that do not exhibit significant diagenetic effects. Diversity varies from 2.20 to 3.02 with a mean value of 2.59. This diversity index is a function of both the number of different species in the assemblage (species richness) and the degree of dominance by those species in the assemblage (evenness). Species richness varies from 36 to 50 species per assemblage count, with a total of 78 different species identified for all the assemblages in this study. There is no significant correlation between richness and $\delta^{13}C$, as indicated by the low correlation coefficient ($r = 0.162$). Evenness shows a strong correlation of -0.65 ($p = 2.8 \times 10^{-17}$) with $\delta^{13}C$, suggesting that both responded to the same phenomenon (Figure 4).

[18] The results of correlation analysis of nannofossil population counts, for species which comprise >5% of the total assemblage in at least some samples, with $\delta^{13}C$ are shown in Table 2. Two species show a strong positive correlation with $\delta^{13}C$: *Zeugrhabdotus moulladei* and *Biscutum constans*. Four taxa have strong negative correlations with carbon isotopic values; the strongest negative correlation is with *Watznaueria barnesiae*, which varies from 3–36% of the total assemblage. It should be noted that in no sample does the abundance of *W. barnesiae* exceed 40% of the assemblage, the point at which *Roth and Bowdler* [1981] suggest significant diagenetic alteration of the assemblage. The other negative correlations are shown by *Tranolithus phacelosus* (including forms that have been attributed to both *T. exiguus* and *T. orionatus*), *Rhagodiscus achylostaurion*, and *Eiffellithus turriseiffeli*.

[19] Principal components analysis of the nannofossil species that account for >5% of at least one assemblage produced a simple one-component model assemblage that explained about 76% of the variance. This component (PCA1) has six important taxa as indicated by their high

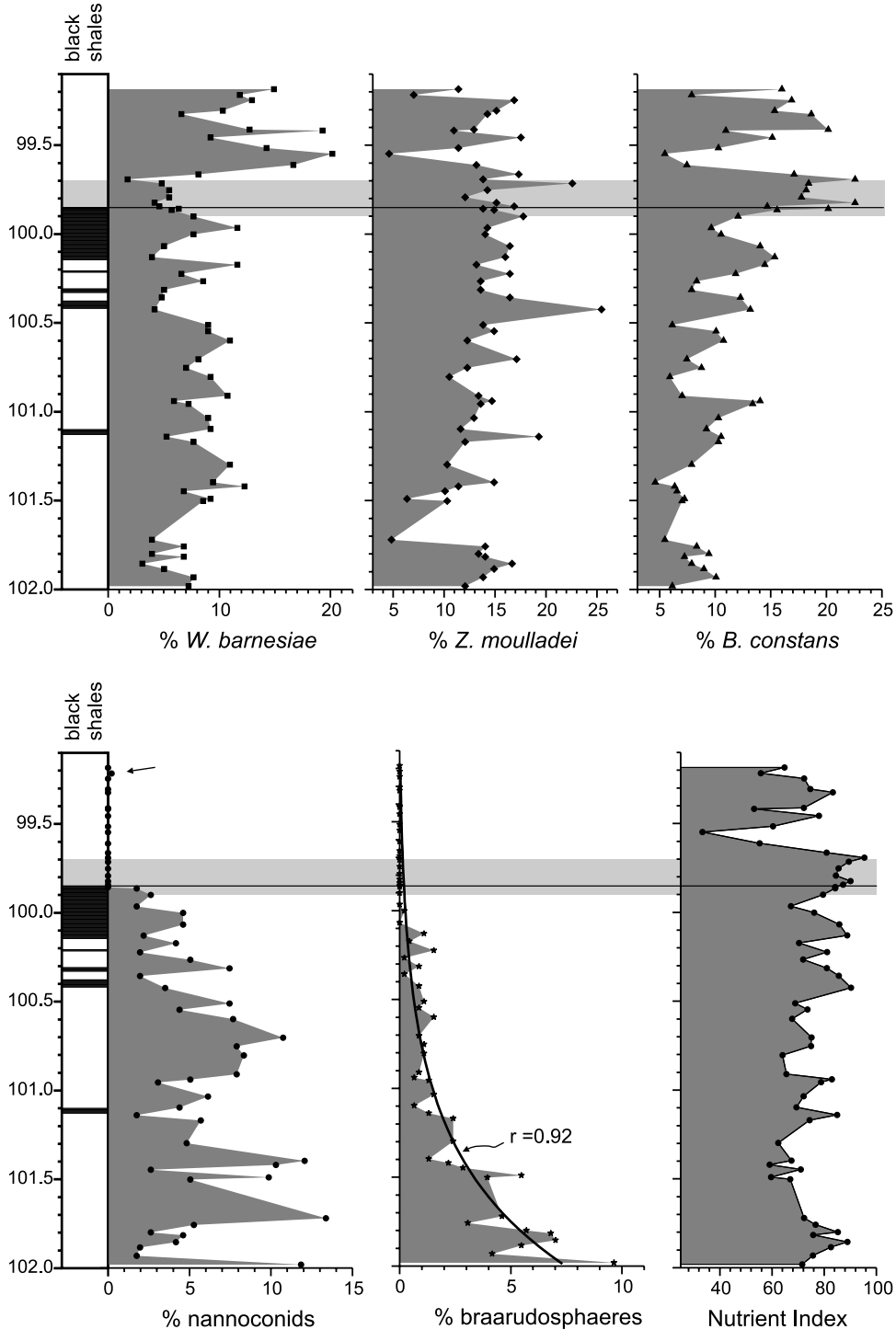

Figure 4. Abundances of major taxa and the nutrient index from the Blake Nose. Disjunct occurrence of nannoconids is indicated by arrow. The distribution of laminated black shale facies, based on data from *Norris et al.* [1998], is illustrated by horizontal shading. The interval of increased extinction (from 99.7 to 99.9 Ma) is indicated by a lighter shaded horizontal band. The level of the maximum positive carbon values in the positive excursion is indicated by a horizontal black line.

component loadings and correlations. Two taxa have strong positive correlations with PCA1: *Biscutum constans* (r = 0.902) and *Zeugrhabdotus moulladei* (0.903). A group of four taxa have significant negative component loadings for PCA1 including *Watznaueria barnesiae* (−0.947), *Eiffellithus turriseiffelii* (−0.771), *Tranolithus phacelosus* (−0.698) and *Rhagodiscus achylostaurion* (−0.670). Carbon isotope values exhibit a strong positive

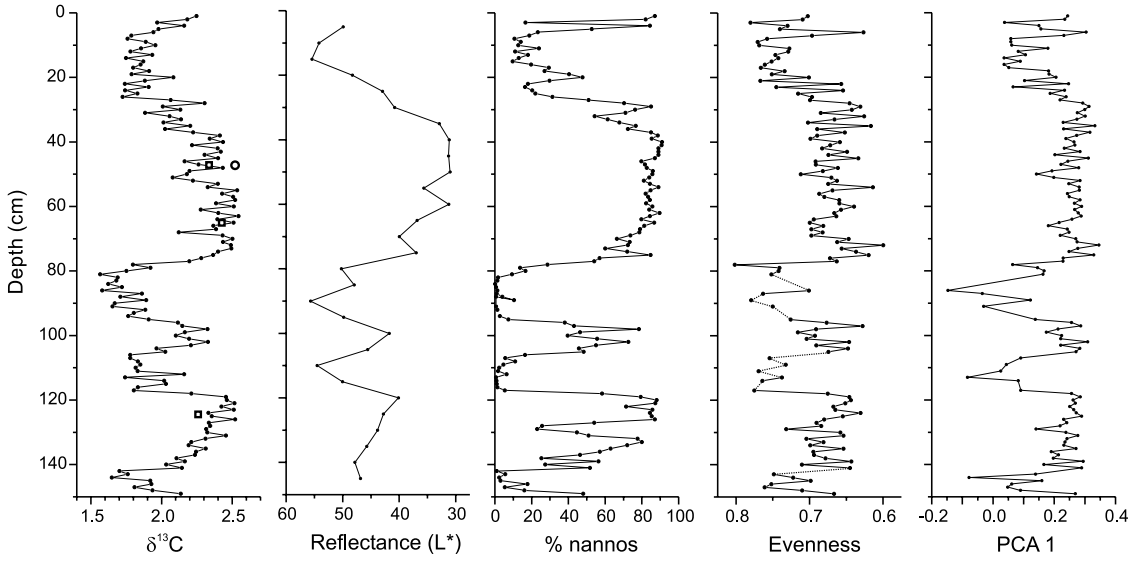

Figure 5. Distribution of carbon isotope values, reflectance, and nannofossil indices in ODP Section 1052E-39R-5. Note that values on the *y* axis for reflectance and nannofossil evenness have been reversed to allow direct comparison with other distributions. Carbon isotope values, plotted as small solid circles connected by line segments, are measured on bulk carbonate. Four $\delta^{13}C$ values measured from discrete, "glassy" well-preserved planktonic foraminiferal calcite in the clay stones [*Wilson and Norris*, 2001] are included for comparison. Three of these discrete values (indicated by squares) are from thermocline-dwelling species, whereas the fourth value (indicated by large open circle) is from a surface-dwelling taxon.

correlation with PCA1 component loadings ($r = 0.70$, $p = 1.0 \times 10^{-20}$, Figure 5).

4. Discussion

4.1. Biostratigraphy

[20] The biostratigraphic succession and the independently derived cyclostratigraphy provide the means to estimate durations of biostratigraphic zones and their calibration to the geochronological timescale. The FAD of *E. turriseiffelii* is used in numerous zonations including the two most widely used schemes, the CC Zonation of *Perch-Nielsen* [1985] and the NC Zonation of *Roth* [1978], where it serves as the base for Zones CC9 and NC10, respectively. The validity of the age estimate of 100.9 Ma is based on recognition of the first appearance of *E. turriseiffelii* s.s. (i.e., large form with symmetrically diagonal crossbars), as stipulated by *Watkins and Bergen* [2003]. *Bralower et al.* [1995] place this first occurrence as approximately coincident with the FAD of the foraminifer *Rotalipora ticinensis* at the base of their integrated Zone IC39. Evidence from Blake Nose suggests that these two events were separated by at least 1 m.y., indicating the possibility of subdividing IC39 by use of the appearance of this strictly defined *E. turriseiffelii*. The base of Subzone CC9b is the LAD of *H. albiensis*, herein estimated at 100.0 Ma. The utility of this species as a biostratigraphic horizon is limited, however, because it is rare in abundance and sporadic in occurrence throughout much of its stratigraphic range (as noted when first proposed as a subzonal marker by *Manivit et al.*, 1977]. *Bralower et al.* [1995] used the FAD of *Gartnerago nanum* as the defining datum for the base of their integrated microfossil zone IC41 of latest Albian age. This datum is estimated at 99.85 Ma, and appears to have coincided almost exactly with the maximum positive values during the OAE1d positive $\delta^{13}C$ excursion. The FAD of *C. kennedyi* is estimated at 99.55 Ma, suggesting that IC42 had a duration of only about 50 k.y. (Figure 2).

4.2. Extinction and Speciation Patterns of Calcareous Nannofossils

[21] Fifteen events (two FADs and thirteen LADs) were concentrated during a relatively short (ca. 200 k.y.) interval in the latest Albian (Figure 2). It is possible that the extinctions were concentrated into a briefer span of time than is implied by the record from Blake Nose. The time interval in question, according to the age model, is represented by approximately 20 m of strata. Many of the species that suffered extinction are rare throughout their ranges, and

Table 2. Results of Correlation Analysis Between the Population of the Principle Species of Nannofossils and Bulk Carbonate $\delta^{13}C$ in Core Section 1052E 39R-5[a]

Taxa	Population, %	*r*	*p*
Zeugrhabdotus moulladei[a]	9–39	0.621	1.4×10^{-15}
Biscutum constans	5–33	0.666	1.9×10^{-18}
Watznaueria barnesiae	3–36	−0.620	1.7×10^{-15}
Tranolithus spp.	1–9	−0.597	3.2×10^{-14}
Rhagodiscus achylostaurion	1–8	−0.571	7.0×10^{-13}
Eiffellithus turriseiffeli	1–7	−0.544	1.3×10^{-11}

[a]See text for further detail.

several become very rare near their last appearance horizon. Abundance levels of the latter are so low as to be difficult to distinguish from reworking, so that their last appearance datums may have been moved upward stratigraphically by bioturbation and/or resedimentation. In addition, the probability of artificial range truncation associated with extinction (Signor-Lipps effect) is increased by the rarity of most of these species [*Signor and Lipps*, 1982]. This brief interval of rapid turnover resulted in a net loss of about ten species (Figure 3) to the richness of the Blake Nose assemblages. This toll would have been higher had two species not had first appearance datums (FAD) in this interval. The two FADs appear to represent the true first appearances of those taxa, as opposed to local migration events. The FAD of *Broinsonia signata* at Blake Nose appears to correlate with the position of this event at Mont Risou, southeast France where they are known from the Breistroffer level [*Gale et al.*, 1996]. This is at a slightly lower stratigraphic position than the lowermost Cenomanian position documented by *Jeremiah* [1996] for southeast England. *Gartnerago nanum* occurs in the lowest sample from Mont Risou documented by *Gale et al.* [1996], corresponding with the base of the Breistroffer level, yielding a minimum estimate for the placement of the FAD. *Bralower and Siesser* [1992] and *Bralower et al.* [1995] place this biostratigraphic event in the uppermost Albian *R. appenninica* foraminiferal Zone, a position approximately equivalent to that at Blake Nose.

[22] Several of the extinction datums appear to correspond with the true stratigraphic ranges of the species. *Nannoconus fragilis* has its last occurrence at 516.6 mbsf in Hole 1052E, equivalent to 99.89 Ma in the age model. *Perch-Nielsen* [1985] cites a similar uppermost Albian last occurrence, suggesting that this is the true extinction of *N. fragilis.* The last occurrence of *Braarudosphaera stenorheta* at Blake Nose is consistent with the highest stratigraphic occurrence of this species in the *M. perinflatum* Subzone of the *S. dispar* ammonite Zone reported by *Jeremiah* [1996], as well as the uppermost Albian LAD in Texas documented by *Hill* [1976]. The last appearance of *Laguncula dorotheae* at Blake Nose is correlative to the highest stratigraphic occurrence of this species at Folkstone, southeast England [*Jeremiah*, 1996].

[23] It is important to note that some of these extinctions may not represent the global extinction of the species. *Calcicalithina alta* and *Isocrystallithus compactus* last occur within OAE1d at Blake Nose, but have ranges that extend well into the lower Cenomanian in the Albian-Cenomanian global boundary stratotype section at Mont Risou, SE France [*Jeremiah*, 1996; *Gale et al.*, 1996]. *Calculites percernis* last occurs within the uppermost Albian on Blake Nose, but is known from the lower Cenomanian the Mont Risou section [*Jeremiah*, 1996]. *Broinsonia stenostaurion* last occurs above the Breistoffer level at Mont Risou [*Gale et al.*, 1996], at a stratigraphic level approximately equivalent to that at Blake Nose, while *Hill* [1976] reports two occurrences in the lower Cenomanian Del Rio Clay. *Zeugrhabdotus streetae* has been only recently described, so its stratigraphic range is poorly documented. As noted by *Kennedy et al.* [2000], however, *Hill* [1976] probably documented the LAD of this species (as *Amphizygus brooksii brooksii*) as lowermost Cenomanian. In addition, several of the taxa that last occurred associated with OAE1d are undescribed (3 *Metadoga* species and *Laguncula* sp. A) or newly described (*Eiffellithus vonsalisiae*) and are documented only from Blake Nose, making it impossible to determine the diachroneity of their extinctions.

[24] Although assessing the global synchroneity of these extinctions and speciations must await detailed investigations from other sections that are well constrained temporally, it is clear that a marked rise in the local extinction rate was associated with OAE1d at Blake Nose. Furthermore, those species that underwent extinction associated with OAE1d shared some common elements. All of these taxa have stratigraphic ranges that are largely or wholly restricted to the Albian. Three taxa (*B. stenostaurion*, *L. dorotheae*, and *Z. streetae*) first appeared in the latest Aptian [*Kennedy et al.*, 2000; *Herrle and Mutterlose*, 2003]. The other ten species are evolutionary products of the well-stratified oceans of the Albian. Most of the species that suffered extinction were relatively rare members of the assemblages, seldom comprising 1% of the assemblage, with the exception of *N. fragilis* and *B. stenorheta*. In addition, there are morphological similarities between several of the taxa that suggest adaptation to specific niches in the water column.

4.3. Depth Zonation of Calcareous Nannofossils

[25] Subtropical regions of the modern north Atlantic and Pacific oceans are characterized by well-developed depth zonation of the calcareous nannoplankton. The warm, well-lit, oligotrophic upper photic zone (approximately 0–80 m water depth) has assemblages that are dominated by *Umbellosphaera irregularis*, *Discosphaera tubifera*, *Rhabdosphaera clavigera*, and is the zone of highest abundance of the holococcoliths. The cooler, dimly lit, but more nutrient-rich lower photic zone is dominated by *Florisphaera profunda* and *Thoracosphaera flabellata* [*Okada and Honjo*, 1973; *Okada and McIntyre*, 1979; *Winter et al.*, 1994].

[26] There is a strong correspondence between the morphology of these modern nannoplankton species and their positions in the water column. The upper photic zone species feature structures that effectively reduce their settling velocities. The spines of *R. clavigera* and *D. tubifera* increase hydrodynamic drag significantly. In the latter species, the spines are salpingiform (trumpet-shaped) processes whose distal expansions substantially increase the apparent diameter of the cell by enveloping a volume of empty space. This significantly increases the apparent volume of the cell while adding little mass, thereby reducing the hydrodynamic density of the cell. An analogous construction is evident in *U. irregularis*, in which the distal shield is greatly expanded to form a salpingiform structure that increases the apparent cell diameter by enclosing empty space. Many of the holococcoliths in the upper photic zone have thin, sometimes perforate, walls enclosing significant empty space. This results in relatively low densities and reduced settling velocities. The dominant taxa of the lower photic zone are both compact, subspherical forms with thick

walls made of numerous overlapping calcite elements that result in a relatively high-density configuration. This heavy construction increases the hydrodynamic density, facilitating the maintenance of a position in the lower photic zone.

[27] There are parallels between the modern forms that exhibit depth zonation and those species that went extinct in the late Albian. The Albian species can be divided into two morphological groups based on the nature of their construction. One group of these taxa consists of four holococcoliths (*I. compactus* and three *Metadoga* species) and two heterococcoliths (*Laguncula dorotheae* and *Laguncula* sp. A) that exhibit expanded, hollow distal processes. These take the form of highly inflated, globular processes in the lagunculas and two of the *Metadoga* species, while *I. compactus* and the other *Metadoga* species have large, hollow cylindrical spines. These forms also are characterized by thin, lightly calicified wall structures. The oversized, inflated processes would have increased the apparent surface area of the coccolithophore, and significantly increased the hydrodynamic drag. The thin-walled, hollow nature of the processes would have increased the volume while adding relatively little mass, effectively reducing the density and, thus the settling velocity. These adaptations toward reduced hydrodynamic density, increased drag, and minimal weight would have been useful for organisms that find it important to maintain a consistent position in the water column. The lightness of construction suggests that these taxa were adapted for the upper part of the surface waters, by analogy with other planktonic organisms.

[28] A second group of species that suffered extinction are characterized by compactly constructed, heavily calcified nannoliths. *Calcicalithina alta* is composed of stacked layers of calcite crystallites that form a solid, rectangular mass. *Braarudosphaera stenorheta* is a distinctive form that is part of a large nannolith consisting of stacked pentagonal units. Postmortem disaggregation of the stacked units yields pentaliths that morphologically differ and have been assigned to *B. stenorheta* and *B. quinquecostata*. For this study, these taxa have been combined as the single taxon *B. stenorheta*. *Nannoconus fragilis* is a heavy, robust, cylindrical nannolith composed of spirally stacked, polygonal calcite crystallites.

[29] *Erba* [1994] posited an analogy between the nannoconids and the modern deep-dwelling *Florisphaera profunda,* citing the similarities in size, gross morphology, heavy calcification, and the antithetic abundance relationship with other coccoliths. In the modern oceans, *F. profunda* occupies the lower photic zone, while most other coccolithophores live higher in the water column. A deep nutricline supplies abundant nutrients to the lower photic zone, allowing *F. profunda* to outproduce the other coccoliths, while a shallow nutricline supplies both *F. profunda* and the other coccoliths, allowing the latter group to outproduce *F. profunda* [*Molfino and McIntyre*, 1990a, 1990b]. By analogy, deep nutricline levels during the mid-Cretaceous would favor nannoconid production, while high nutricline levels would favor other coccoliths [*Erba*, 1994; *Herrle*, 2003].

[30] Nannoconids are common to abundant throughout the lower and middle part of the mid-Cretaceous section in ODP Hole 1052E, where they generally comprise 2–8% of the assemblages, and with four abundance peaks that exceed 10% (Figure 4). They are absent from samples above 99.87 Ma (513.28 mbsf) except for one rare occurrence. *Nannoconus fragilis* has its last occurrence at about 99.89 Ma (516.57 mbsf), while *Nannoconus truittii* continues higher in the section, albeit as rare occurrences, until its local disappearance at about 99.82 Ma (507.57 mbsf). The latter species reappears in a single sample in the Cenomanian (marked by arrow in Figure 4), but at abundance levels so low as to be indistinguishable from reworking. *Nannoconus truitii* is known to continue until the Campanian in other areas [e.g., *Perch-Nielsen*, 1985], and thus its extinction on Blake Nose is a local exclusionary event. Indeed, there is a rich assemblage (5–10 species) of nannoconids reported from the post-OAE1d Albian and lower Cenomanian of the Vocontian Basin, southeast France [*Jeremiah*, 1996; *Gale et al.*, 1996]. It is clear that this local exclusionary event was the result of the loss of habitat for nannoconids in this region during and immediately after the stratification collapse associated with OAE1d.

[31] Reconstructions of the *Braarudosphaera* skeleton by *Lambert* [1986] indicate that the encystment structure would have been a heavily armored, spiny sphere analogous to the nannoconid skeleton. The similarities in size, gross morphology, heavy degree of calcification, and hydrodynamic density between braarudosphaeres and nannoconids suggest that they could have shared a similar, deep photic (thermocline) habitat during some phase of their life cycles. Braarudosphaeres are relatively abundant in the lower part of the section (prior to about 101.4 Ma), where they comprise 4–10% of the total nannofossil assemblages (Figure 4). Their abundance drops to 1–3% in the middle of the section, corresponding to 100 to 101.4 Ma in the age model. This species has its last occurrence near the base of OAE1d in Holes 1050C and 1052E, at a level that is dated at 99.87 Ma. This extinction level appears to correspond precisely with the LAD of *B. stenorheta* reported by *Hill* [1976] from the Paw Paw Shale of the Texas upper Albian.

[32] The accelerated extinction rate associated with OAE1d, and the unusual morphologies of nine of the thirteen extinct species, suggests a causal link between the extinctions and the paleoceanographic evolution of the area. Oxygen isotopic evidence indicates that the Blake Nose region was characterized by an increasingly warm and well-stratified upper water column throughout most of the middle and late Albian [*Leckie et al.*, 2002]. The well-stratified nature of the upper water column partitioned the photic zone into a series of relatively stable niches that were exploited by adaptive radiation of these unusual nannoplankton. Compact, heavily calcified morphotypes occupied niche space near the base of the photic zone, where a deep nutricline would supply abundant nutrients to offset the penalty of low light levels on growth and reproduction. Inflated, lightly calcified forms probably occupied the niche space high in the upper water column, in well-lit but (probably) oligotrophic conditions. Collapse of the upper water stratification, as evident from oxygen isotope time series in planktonic foraminiferal calcite [*Wilson and Norris*, 2001], homogenized the upper surface water col-

umn, temporarily eliminating the partitioned niche spaces at the top and base of the photic zone. The elimination of their niche space led to the extinction of these unusual forms and a general drop in the species richness of the assemblages in this area.

[33] *Leckie et al.* [2002] derived the rates of speciation and extinction of calcareous nannofossil associated with mid-Cretaceous OAEs using a database of 78 species with well-documented stratigraphic ranges. No calcareous nannofossil speciation or extinction was reported for OAE1d. Given the appropriately conservative nature of the database, they are correct in their assertion. The record from Blake Nose indicates that no long-ranging, relatively common species evolved or became extinct associated with OAE1d. Instead, OAE1d appears to have been an extinction episode for rare, short-ranging forms that had evolved as specialists exploiting restricted niches in the well-stratified late Albian ocean, and suffered extinction when these niche spaces disappeared during stratification collapse.

4.4. Surface Water Fertility

[34] *Zeugrhabdotus moulladei* is widely cited as an indicator of elevated fertility based on abundance in inferred upwelling areas [*Roth and Bowdler*, 1981; *Roth and Krumbach*, 1986; *Erba*, 1992] and in rocks with high organic carbon contents [*Watkins*, 1986, 1989; *Premoli Silva et al.*, 1989; *Erba et al.*, 1992]. Quantitative analysis of mid-Cretaceous, equatorial Pacific Ocean assemblages suggest that *Z. moulladei* preferred more eutrophic surface waters than other taxa (most notably *B. constans* [*Erba et al.*, 1992; *Erba*, 1992]. At Blake Nose, there is no clear trend in the distribution of *Z. moulladei*, although three abundance peaks correspond with black shale deposition and with the rapid extinction episode above OAE1d (Figure 4). The correspondence of the abundance peaks with black shales at Site 1052 suggests that these intervals may represent the highest surface water fertility in the sequence.

[35] Elevated abundances of *B. constans* have been linked to high surface water fertility by numerous quantitative studies of assemblages from various mid-Cretaceous oceanic and epicontinental settings [*Roth*, 1981, 1986, 1989; *Roth and Bowdler*, 1981; *Roth and Krumbach*, 1986; *Erba*, 1992; *Erba et al.*, 1992; *Premoli Silva et al.*, 1989; *Watkins*, 1989]. Studies indicate that *B. constans* was most abundant in oceanic surface waters with moderately elevated (mesotrophic) fertility [*Erba*, 1992; *Erba et al.*, 1992]. *Biscutum constans* exhibits a relatively clear progressive increase in abundance leading up to OAE1d (Figure 4). This is especially marked from 100.9 to 99.9 Ma, which was characterized by a series of increasingly higher minima and maxima, culminating in the highest values associated with the latter part of OAE1d and the rapid extinction episode. This suggests that average fertility levels progressively increased during the one million years prior to the collapse of upper water column stratification associated with OAE1d.

[36] The most striking feature of the distribution of *W. barnesiae* through the section is the marked increase in abundance that occurs associated with the end of the rapid extinction episode and the Albian/Cenomanian boundary (Figure 4). The abundance of *W. barnesiae* has been related to low-fertility conditions in the mid-Cretaceous in several studies [*Roth and Krumbach*, 1986; *Erba et al.*, 1992; *Williams and Bralower*, 1995; *Herrle*, 2002; *Herrle et al.*, 2003a, 2003b]. The distribution of *W. barnesiae* at Blake Nose suggests that surface water fertility was relatively higher in the late Albian, and then significantly decreased in the early Cenomanian, especially just above the Albian/Cenomanian boundary.

[37] Both braarudosphaerids and nannoconids exhibited well-defined, progressive decreases in abundance from their highest values (101.4 to 102 Ma) to their extinction or local exclusion during OAE1d (Figure 4). Assuming that they occupied a niche in the lower photic zone, as discussed above, these trends suggest that there was increasing instability in the lower photic zone from about 101.4 Ma until the complete collapse of the surface water stratification associated with OAE1d.

[38] As noted above, the three most abundant taxa in these assemblages have been interpreted elsewhere as fertility indicators, with *Z. moulladei* abundant under eutrophic conditions, *B. constans* abundant under mesotrophic conditions, and *W. barnesiae* dominant under oligotrophic conditions. Given the well-documented nature of their paleoecological affinities, the abundances of these three taxa are used to construct a nutrient index following the manner of *Herrle et al.* [2003a]. This index is the ratio of the abundances of the two elevated fertility species divided by the sum of the abundances for all three taxa as follows:

$$\text{N.I.} = [(\text{Bc} + \text{Zm})/(\text{Bc} + \text{Zm} + \text{Wb})]100$$

where Bc = *B. constans*, Zm = *Z. moulladei*, and Wb = *W. barnesiae*. The stratigraphic distribution of the nutrient index (Figure 4) suggests a progressive rise in fertility from about 101 Ma to a culmination during the interval of rapid extinction (99.7 to 99.9 Ma), followed by a rapid decline to the lowest levels associated with the Albian/Cenomanian boundary. A recovery to moderate levels followed during the early Cenomanian.

[39] Analysis of the distribution of major taxa suggests an internally consistent history of surface water fertility changes during the late Albian and early Cenomanian of Blake Nose. The deposition of the first black shale at approximately 101.1 Ma was accompanied by a peak in *Z. moulladei* and, to a lesser extent, *B. constans* and a minimum in nannoconids, suggesting that a brief pulse of higher surface water fertility was associated with this black shale. The interval from approximately 100.9 to 99.9 Ma was characterized by a gradual rise in fertility (N.I.) and instability of the deeper surface water (decline of nannoconids and braarudospheres), although a significant variation in values characterized this interval (Figure 4). This interval was also characterized by a gradually increasing thermocline temperature and a variable, but generally decreasing, SST (Figure 2) [*Wilson and Norris*, 2001]. Surface water fertility attained maximum values during the waning phases of OAE1d black shale deposition and continued above the maximum positive carbon isotope excursion through the rapid extinction episode. There was a relatively rapid drop

in fertility above the rapid extinction episode, associated with the Albian/Cenomanian boundary (99.6 Ma), followed by a recovery back to moderate fertility levels in the early Cenomanian.

4.5. Precessional Cycles

[40] Numerical analysis of the diversity data indicates that the species richness has little importance in the variation of diversity, and that the strong negative correlation with bulk sediment $\delta^{13}C$ is a function of changes in evenness (Figure 5). High evenness values indicate a stable, oligotrophic condition with reduced dominance in the assemblage and elevated abundances of k-selected (specialists) taxa. Low evenness values are associated generally with unstable, mesotrophic to eutrophic environments and dominance by a few r-selected (opportunists) taxa. In section 1052E-39R-5, the limestones and marlstones that show high evenness values show low bulk sediment $\delta^{13}C$ (generally <2‰) whereas the dark clay stones with lower evenness values show relatively high (>2.2‰) $\delta^{13}C$. This observation suggests cyclical changes in the strength of the biological pump indicating that the carbonate-rich sediments were deposited during intervals of lower surface water fertility and organic productivity than the carbonate-poor sediments. Yet modern coccoliths show extreme species-dependent fractionation (+3‰ to −2.5‰ [*Ziveri et al.*, 2003]) calling into question interpretations of changes in surface water chemistry based on bulk sediment $\delta^{13}C$. In contrast, the Cretaceous nannofossil carbonate that we have analyzed appears to have grown in near-isotopic equilibrium with parent seawater because bulk sediment $\delta^{13}C$ is close to $\delta^{13}C$ measured in "glassy" well-preserved planktonic foraminiferal calcite in the clay stones [*Wilson and Norris*, 2001] (Figure 5). This gives us confidence to interpret the changes seen in bulk sediment $\delta^{13}C$ as an environmental signature.

[41] Correlation analysis and principle components analysis identifies the six species that have strong correlation with $\delta^{13}C$. Five of these six taxa have been identified by other studies as having probable relationships with surface water fertility. *Zeugrhabdotus moulladei* and *Biscutum constans* are widely cited as indicators of elevated fertility, while *W. barnesiae* appears to have preferred oligotrophic conditions during the mid-Cretaceous (as discussed above). Elevated abundances of *Eiffellithus turriseiffelii* and *Tranolithus phacelosus* were used by *Watkins* [1989] to indicate lower surface water fertility, based upon their positive correlation with Shannon diversity and their negative correlations with *B. constans* and *Z. moulladei* in upper Cenomanian rocks associated with OAE2.

[42] The clear dominance of PCA1 by species that are known to relate to surface fertility, and the fact that indicator species for elevated fertility have a positive correlation with PCA1 while low fertility indicator species have negative correlations with PCA1, indicates that PCA1 is a fertility indicator. Calculation of a nutrient index for these samples indicates a near perfect correlation ($r = 0.98$, $p < 1 \times 10^{-100}$) between PCA1 and the nutrient index. The strong correlation between $\delta^{13}C$ and PCA1 ($r = 0.7$, $p = 1 \times 10^{-20}$) indicates that both are reacting similarly to a common causal mechanism. Higher values of carbon isotopes, indicating greater biogenic sequestration of carbon in the upper water column, correlate to higher values of surface water fertility, as measured by PCA1.

[43] The strong correspondence of nannofossil evenness, nannofossil fertility, and $\delta^{13}C$ with sedimentary cycles (alternations of light limestones and dark marlstones) indicates that these rock cycles are manifestations of cyclically varying productivity in the surface water column. We suggest that these productivity changes are the result of variations in the strength of upwelling or deep winter mixing, with intensified upwelling and winter mixing of intermediate and surface waters resulting in higher productivity, enhanced carbon burial, darker sediment, and more highly dominated nannofossil assemblages rich in *B. constans* and *Z. moulladei*.

[44] The response of the nannofossil assemblages (characterized by evenness and PCA1) to changes in the physical environment (as indicated by the carbon isotope proxy) is rapid and shows no detectable lag time between environmental change and assemblage response (Figure 5). This synchronous response, as indicated by the high correlation of carbon isotopes to PCA1 ($r = 0.70$, $p < 1 \times 10^{-20}$) and to evenness ($r = -0.65$, $p < 2.8 \times 10^{-17}$), indicates a relatively low degree of resistance and a high degree of elastic resilience in the paleocommunity to change of environmental conditions. The changes in abiotic factors accompanying the precessional cycles were well within the amplitude resilience of the community. It was only during collapse of the vertical stratification that the amplitude resilience of the community was exceeded, permanently changing the structure of the assemblage to the point that it could not reestablish itself at the former equilibrium state.

[45] There is a wide variation in the percentage of nannofossils in the carbonate fraction (Figure 5) from <1% to >90%. There appears to have been an upper limit of approximately 91% coccolith carbonate, suggesting a limit of approximately 10:1 in the abundance relationship between coccolith and planktonic foraminifera in terms of carbonate production. This ratio is similar to that predicted by trophic theory, suggesting an irreducible ratio of phytoplankton to zooplankton even during intervals of elevated organic productivity. On the other hand, there are numerous samples dominated by other carbonate, with coccolith carbonate content of <1%. Coccoliths from samples of very low percentage of nannofossils exhibit significant etching (E2-E3) and moderate overgrowth, suggesting that diagenetic destruction is responsible, at least in part, for their rarity. There is little evidence of significant alteration of coccoliths in those samples with more than 10% coccoliths, however, indicating that much of the variation in nannofossil content is a primary feature. This is especially true in samples with >50% nannofossil, because the majority of other grains retain sufficient primary microstructure to identify their planktonic foraminiferal origins.

[46] Two possibilities exist to explain the correlations of nannofossil content, $\delta^{13}C$, and nannofossil fertility and diversity indices. The first is that, despite the qualitative evidence against significant diagenesis of nannofossils in most samples, the relationships are driven by diagenetic changes in carbonate distribution in the sediment. Yet the

amplitude of $\delta^{13}C$ cycles seen in our records is large in comparison to that readily attributable to diagenetic alteration [*Frank et al.*, 1999]. The second possible explanation is that the carbon isotopes and nannofossil indices indicate high surface water fertility and upwelling during deposition of the dark shale. These oceanographic conditions, with the attendant surface water instability and low oxygen content (expanded OMZ), progressively depressed the abundance of planktonic foraminifers.

4.6. Comparison to Other Aptian-Albian OAEs

[47] The early Aptian OAE1a (=Selli Level) was a global event [e.g., *Erba*, 1992] characterized by a significant (>2‰) positive carbon isotope shift and a significant impact of the planktonic communities. Radiolarians exhibited significant extinction (26% of assemblage) and replacement by speciation (41% of assemblage) associated with OAE1a [*Erbacher and Thurow*, 1997]. Planktonic foraminifers had a speciation rate of 22% leading up to OAE1a and an extinction rate of 27% following OAE1a [*Leckie et al.*, 2002], although *Premoli Silva et al.* [1999] found no planktonic foraminiferal extinctions associated directly with OAE1a. Nannofossils experienced a 7% turnover, according to *Leckie et al.* [2002], but evidence from SE France suggests a greater impact on the assemblages [*Herrle and Mutterlose*, 2003]. In addition to species turnover, OAE1a had a significant effect on the paleoecological nature of the nannofossil assemblages.

[48] *Erba* [1994] documented the dramatic change of nannoconids as a proportion of the assemblages associated with OAE1a, with pre-OAE1a nannoconid abundance levels of 20–60% decreasing to zero or near-zero levels during OAE1a, and only recovering partially following OAE1a. *Erba* [1994] attributed this "nannoconid crisis" to upward migration of the nutricline during the anoxic event. There are several parallels between the situation documented by *Erba* [1994] for the lower Aptian OAE1a and that associated with the upper Albian OAE1d on Blake Nose. Although the precrisis nannoconid abundance levels in the Aptian were significantly higher (10–60%) than the corresponding ones for the upper Albian (2–10%), both cases exhibit rapid declines in abundance at or just before the onset of the OAE. Comparison of the Aptian Cismon Section [*Erba*, 1994] and the Albian Blake Nose records indicates that the declines corresponded with the start of a significant positive $\delta^{13}C$ anomaly.

[49] The early Albian OAE1b was apparently manifest on a regional scale encompassing the western Tethys and North Atlantic [*Erbacher et al.*, 2001]. Biotic effects were spread over a broader time frame, but there still seems to have been significant turnover in the radiolarians [*Erbacher and Thurow*, 1997] and planktonic foraminifers [*Leckie et al.*, 2002]. No turnover of calcareous nannofossil species is reported by *Leckie et al.* [2002], although evidence from southeast France suggests some extinctions and speciations associated with OAE1b [*Herrle and Mutterlose*, 2003].

[50] There is abundant evidence that OAE1b (early Albian) was significantly different in genesis from OAE1a and OAE1d. An examination of OAE1b (Niveau Paquier) in the Vocontian Basin of southeast France reveals the opposite relationship to that of OAE1a and OAE1d, with nannoconids abundant (>10%) only during OAE1b and rare or absent in the adjacent strata [*Herrle*, 2002, 2003). Similarly, braarudospheres (in this case, *B. africana*) are only present during OAE1b. There is a prominent negative carbon isotope shift of about 1.5‰ associated with OAE1b in the Vocontian Trough of France [*Herrle*, 2002, 2004] and Blake Nose [*Erbacher et al.*, 1999], and a somewhat smaller negative carbon isotope shift of about 1.2‰ recorded from the Mazagan Plateau (DSDP Site 545) of the eastern North Atlantic [*Herrle et al.*, 2004]. *Erbacher et al.* [2001] propose that an increase in surface water temperatures and runoff caused decreased bottom water formation and formation of a "super sapropel" in the western Tethys and North Atlantic. The resultant stratification of the water column during OAE1b led to enhanced carbon sequestration and provided niche space for the braarudospheres and nannoconids near the thermocline.

5. Conclusions

[51] The calcareous nannofossil succession from the upper Albian and lower Cenomanian of Blake Nose, and its correlation to the age model derived from cyclostratigraphy, provides the means to estimate the geochronological age of several important biostratigraphic datums. Assuming the age of the Albian/Cenomanian boundary as 99.6 Ma, estimates for zonal marker horizons include: FAD *C. kennedyi* at 99.55 Ma, FAD *G. nanum* at 99.85 Ma, LAD *H. albiensis* at 100.03 Ma, and FAD *E. turriseiffelii* at 100.95 Ma. In addition, this age model estimates the LAD of the planktonic foraminifer *R. appenninica* at 100.12 Ma, and (by definition) FAD of *R. globotruncanoides* at 99.6 Ma (Table 1).

[52] Thirteen taxa underwent extinction at Blake Nose associated with OAE1d. There is evidence that some of these extinctions were local or regional in extent (e.g., *C. alta*), whereas others appear to correspond to ranges published from other localities (e.g., *N. fragilis*, *B. stenorheta*). All of these taxa evolved in the late Aptian and Albian, when the upper water column was moderately to well-stratified. Most of these species were rare prior to the extinction, with the exception of the braarudospheres and the nannoconids. Nine of the thirteen taxa had morphological features that appear to have been adaptations to maintaining a preferred position in the water column. The nearly simultaneous extinction of these paleoecologically related forms suggests that the disruption of upper water stratification led to the disappearance (at least temporarily) of their preferred niche space.

[53] The distribution of major taxa through the section at Blake Nose suggests that the collapse of upper water column stratification associated with OAE1d was preceded by approximately 1 m.y. of increasingly higher surface water fertility and water column variability and instability. Progressive increases in the maximum abundance of the mesotrophic indicator species *B. constans*, coupled with concomitant decreases in the oligotrophic indicator species *W. barnesiae*, suggest strengthening upwelling and/or deep mixing of surface and intermediate water masses during this

interval. This is expressed as the trend toward increasing values of the nutrient index through this interval. The progressive diminution of probable thermocline dwellers such as the nannoconids and braarudospheres suggest increasing instability of the thermocline through this interval. These patterns of abundance are consistent with the isotopic record indicating increasing thermocline temperatures, variable and generally decreasing SST's, and progressive reduction in the vertical thermal gradient in the upper water column.

[54] Detailed investigation of ODP Section 1052E-39R-5 indicates a strong positive correlation of bulk carbonate $\delta^{13}C$, percent nannofossils, and surface fertility (as indicated by PCA1, the fertility component), and their strong negative correlations with sediment lightness (as expressed by reflectance) and nannofossil assemblage evenness. The close correspondence of these proxies suggests orbitally paced changes in the strength of deep mixing of surface and intermediate waters and/or the upwelling of nutrient-rich waters in the western North Atlantic during the late Albian.

[55] **Acknowledgments.** This research used samples and data provided by the Ocean Drilling Program. The ODP is sponsored by the U.S. National Science Foundation (NSF) and participating countries under management of Joint Oceanographic Institutions (JOI), Inc. Funding for this research was provided by JOI-USSAC and National Science Foundation grant 9910025 to D.K.W. This work was supported by a NERC grant to P.A.W. This manuscript was improved significantly by comments from Jens Herrle and by the formal reviews of R. Mark Leckie and Timothy J. Bralower.

References

Arthur, M. A., S. O. Schlanger, and H. C. Jenkyns (1987), The Cenomanian-Turonian oceanic anoxic event II, Paleoceanographic controls on organic matter production and preservation, in *Marine Petroleum Source Rocks*, edited by J. Brooks and A. Fleet, *Geol. Soc. Spec. Publ.*, *26*, 399–418.

Arthur, M. A., H.-J. Brumsack, H. C. Jenkyns, and S. O. Schlanger (1990), Stratigraphy, geochemistry, and paleoceanography of organic carbon-rich Cretaceous sequences, in *Cretaceous Resources, Events, and Rhythms*, edited by R. N. Ginsburg and B. Beaudoin, pp. 75–119, Springer, New York.

Bellier, J. P., M. R. Moullade, and B. T. Huber (2001), Mid-Cretaceous planktonic foraminifers from Blake Nose: Revised biostratigraphic framework, *Proc. Ocean Drill. Program Sci. Results*, *171B*, 1–12.

Bralower, T. J., and W. G. Siesser (1992), Cretaceous calcareous nannofossil biostratigraphy of sites 761, 762, and 763 Exmouth and Wombat plateaus, northwest Australia, *Proc. Ocean Drill. Program Sci. Results*, *122*, 529–556.

Bralower, T. J., M. A. Arthur, R. M. Leckie, W. V. Sliter, D. Allard, and S. O. Schlanger (1994), Timing and paleoceanography of oceanic dysoxia/anoxia in the late Barremian and early Aptian, *Palaios*, *9*, 335–369.

Bralower, T. J., R. M. Leckie, W. V. Sliter, and H. R. Thierstein (1995), An integrated Cretaceous microfossil biostratigraphy, *Spec. Publ. SEPM, Soc. Sediment. Geol.*, *54*, 65–79.

Erba, E. (1992), Middle Cretaceous calcareous nannofossils from the western tropical Pacific (ODP Leg 129): Evidence for paleoequatorial crossings, *Proc. Ocean Drill. Program Sci. Results*, *129*, 189–201.

Erba, E. (1994), Nannofossils and superplumes: The early Aptian "nannoconid crisis," *Paleoceanography*, *9*, 483–501.

Erba, E., D. Castradori, G. Guasti, and M. Ripepe (1992), Calcareous nannofossils and Milankovitch cycles: The example of the Albian Gault Clay Formation (southern England), *Palaeogeogr. Palaeoclimatol. Palaeoecol.*, *93*, 47–69.

Erbacher, J., and J. Thurow (1997), Influence of oceanic anoxic events on the evolution of mid-Cretaceous radiolaria in the North Atlantic and western Tethys, *Mar. Micropaleontol.*, *30*, 139–158.

Erbacher, J., J. Thurow, and R. Littke (1996), Evolution patterns of radiolaria and organic matter variations: A new approach to identify sea-level changes in mid-Cretaceous pelagic environments, *Geology*, *24*, 499–502.

Erbacher, J., C. Hemleben, B. T. Huber, and M. Markey (1999), Correlating environmental changes during early Albian oceanic anoxic event 1b using benthic foraminiferal paleoecology, *Mar. Micropaleontol.*, *38*, 7–28.

Erbacher, J., B. T. Huber, R. D. Norris, and M. Markey (2001), Increased thermohaline stratification as a possible cause of an oceanic anoxic event in the Cretaceous period, *Nature*, *409*, 325–327.

Fassell, M. L., and T. J. Bralower (1999), Warm, equable mid-Cretaceous: Stable isotope evidence, *Spec. Pap. Geol. Soc. Am.*, *332*, 121–142.

Frank, T. D., M. A. Arthur, and W. E. Dean (1999), Diagenesis of Lower Cretaceous pelagic carbonates, North Atlantic: Paleoceanographic signals obscured, *J. Foraminiferal Res.*, *29*, 340–351.

Gale, A. S., W. J. Kennedy, J. A. Burnett, M. Caron, and B. E. Kidd (1996), The late Albian to early Cenomanian succession at Mont Risou near Rosans (Drome, SE France): An integrated study (ammonites, inoceramids, planktonic foraminifera, nannofossils, oxygen and carbon isotopes), *Cretaceous Res.*, *17*, 515–606.

Gradstein, F. M., J. G. Ogg, A. G. Smith, W. Bleeker, and L. Lourens (2004), A new geological time scale with special reference to Precambrian and Neogene, *Episodes*, *27*, 83–100.

Hammer, Ø., D. A. T. Harper, and P. D. Ryan (2001), PAST: Paleontological Statistics Software Package for Education and Data Analysis, *Palaeontol. Electron.*, *4*(1), article 4.

Herrle, J. O. (2002), Paleoceanographic and paleoclimatic implications on mid-Cretaceous black shale formation in the Vocontian Basin and the Atlantic: Evidence from calcareous nannofossils and stable isotopes, *Tubinger Mikropalaontol. Mitt.*, *27*, 1–114.

Herrle, J. O. (2003), Reconstructing nutricline dynamics of mid-Cretaceous oceans: Evidence from calcareous nanofossils from the Niveau Paquier black shale (SE France), *Mar. Micropaleontol.*, *47*, 307–321.

Herrle, J. O., and J. Mutterlose (2003), Calcareous nannofossils from the Aptian and lower Albian of southeast France: Palaeocological and biostratigraphic implications, *Cretaceous Res.*, *24*, 1–22.

Herrle, J. O., J. Pross, O. Fredrich, P. Kobler, and C. Hemleben (2003a), Forcing mechanisms for mid-Cretaceous black shale formation: Evidence from the upper Aptian and lower Albian of the Vocontian Basin (SE France), *Palaeogeogr. Palaeoclimatol. Palaeoecol.*, *190*, 399–426.

Herrle, J. O., J. Pross, O. Friedrich, and C. Hemleben (2003b), Short-term environmental changes in the Cretaceous Tethyan Ocean: Micropaleontological evidence from the early Albian oceanic anoxic event 1b, *Terra Nova*, *15*, 14–19.

Herrle, J. O., P. Kobler, O. Friedrich, H. Erlenkeuser, and C. Hemleben (2004), High-resolution carbon isotope records of the Aptian to lower Albian from SE France and the Mazagan Plateau (DSDP Site 545), A stratigraphic tool for paleoceanographic and paleobiologic reconstruction, *Earth Planet. Sci. Lett.*, *218*, 149–161.

Hill, M. E., III (1976), Lower Cretaceous calcareous nannofossils from Texas and Oklahoma, *Palaeontogr., Abt. B*, *156*, 103–179.

Huber, B. T., R. M. Leckie, R. D. Norris, T. J. Bralower, and E. CoBabe (1999), Foraminiferal assemblage and stable isotopic change across the Cenomanian-Turonian boundary in the subtropical North Atlantic, *J. Foraminiferal Res.*, *29*, 392–417.

Jeremiah, J. (1996), A proposed Albian to lower Cenomanian nannofossil biozonation for England and the North Sea basin, *J. Micropalaeontol.*, *15*, 97–129.

Kennedy, W. J., A. S. Gale, P. R. Bown, M. Caron, R. J. Davey, D. Groecke, and D. S. Wray (2000), Integrated stratigraphy across the Aptian-Albian boundary in the Marnes Bleues, at the Col de Pre-Guittard, Arnayon (Drome), and at Tartonne (Alpes-de-Haute-Provence), France: A candidate global boundary stratotype section and boundary point for the base of the Albian stage, *Cretaceous Res.*, *21*, 591–720.

Lambert, B. (1986), La notion d'espece chez le genre *Braarudosphaera* Deflandre, 1947: Mythe et realite, *Rev. Micropaleontol.*, *28*, 255–264.

Leckie, R. M., T. J. Bralower, and R. Cashman (2002), Oceanic anoxic events and plankton evolution: Biotic response to tectonic forcing

during the mid-Cretaceous, *Paleoceanography*, *17*(3), 1041, doi:10.1029/2001PA000623.

Manivit, H., K. Perch-Nielsen, B. Prins, and J. W. Verbeek (1977), Mid Cretaceous calcareous nannofossil biostratigraphy, *Proc. K. Ned. Akad. Wet., Ser. B Palaeontol. Geol. Phys. Chem.*, *80*, 169–181.

Molfino, B., and A. McIntyre (1990a), Precessional forcing of nutricline dynamics in the equatorial Atlantic, *Science*, *24*, 766–769.

Molfino, B., and A. McIntyre (1990b), Nutricline variation in the equatorial Atlantic coincident with the Younger Dryas, *Paleoceanography*, *5*, 997–1008.

Norris, R. D., and P. A. Wilson (1998), Low-latitude sea-surface temperatures for the mid-Cretaceous and the evolution of planktic foraminifera, *Geology*, *26*, 823–826.

Norris, R. D., D. Kroon, and A. Klaus (Eds.) (1998), *Proceedings of the Ocean Drilling Program Initial Results*, vol. 171B, Ocean Drill. Program, College Station, Tex.

Norris, R. D., K. L. Bice, E. A. Mango, and P. A. Wilson (2002), Jiggling the tropical thermostat in the Cretaceous hothouse, *Geology*, *30*, 299–302.

Okada, H., and S. Honjo (1973), The distribution of oceanic coccolithophorids in the Pacific, *Deep Sea Res. Oceanogr. Abstr.*, *20*, 355–374.

Okada, H., and A. McIntyre (1979), Seasonal distribution of modern coccolithophores in the western North Atlantic Ocean, *Mar. Biol.*, *54*, 319–328.

Perch-Nielsen, K. (1985), Mesozoic calcareous nannofossils, in *Plankton Stratigraphy*, edited by H. M. Bolli, J. B. Saunders, and K. Perch-Nielsen, pp. 329–426, Cambridge Univ. Press, New York.

Premoli Silva, I., E. Erba, and M. E. Tornaghi (1989), Paleoenvironmental signals and changes in surface fertility in mid Cretaceous corg-rich pelagic facies of the fucoid marls (central Italy), *Geobios*, *11*, 225–236.

Premoli Silva, I., E. Erba, G. Salvini, C. Locatelli, and D. Verge (1999), Biotic changes in Cretaceous oceanic anoxic events of the Tethys, *J. Foraminiferal Res.*, *29*, 352–370.

Roth, P. R. (1978), Cretaceous nannoplankton biostratigraphy and oceanography of the northwestern Atlantic Ocean, *Initial Rep. Deep Sea Drill. Proj.*, *44*, 731–759.

Roth, P. H. (1981), Mid-Cretaceous calcareous nannoplankton from the central Pacific: Implications for paleoceanography, *Initial Rep. Deep Sea Drill. Proj.*, *62*, 471–489.

Roth, P. H. (1986), Mesozoic palaeoceanography of the North Atlantic and Tethys oceans, in *North Atlantic Palaeoceanography*, edited by C. P. Summerhayes and N. J. Shackleton, *Geol. Soc. Spec. Publ. London*, *21*, 299–320.

Roth, P. H. (1989), Ocean circulation and calcareous nannoplankton evolution during the Jurassic and Cretaceous, *Palaeogeogr. Palaeoclimatol. Palaeoecol.*, *74*, 111–126.

Roth, P. H., and J. L. Bowdler (1981), Middle Cretaceous calcareous nannoplankton biostratigraphy and oceanography of the Atlantic Ocean, *Spec. Publ. Soc. Econ. Paleontol. Mineral.*, *32*, 517–546.

Roth, P. H., and K. R. Krumbach (1986), Middle Cretaceous calcareous nannofossil biogeography and preservation in the Atlantic and Indian oceans: Implications for paleoceanography, *Mar. Micropaleontol.*, *10*, 235–266.

Signor, P. W., and J. H. Lipps (1982), Sampling bias, gradual extinction patterns and catastrophes in the fossil record, *Geol. Soc. Am. Spec. Pap.*, *190*, 291–296.

Watkins, D. K. (1986), Calcareous nannofossil paleoceanography of the Cretaceous Greenhorn Sea, *Geol. Soc. Am. Bull.*, *97*, 1239–1249.

Watkins, D. K. (1989), Nannoplankton productivity fluctuations and rhythmically-bedded pelagic carbonates of the Greenhorn Limestone (Upper Cretaceous), *Palaeogeogr. Palaeoclimatol. Palaeoecol.*, *74*, 75–86.

Watkins, D. K., and J. A. Bergen (2003), Late Albian adaptive radiation in the calcareous nannofossil genus *Eiffellithus*, *Micropaleontology*, *49*, 231–252.

Watkins, D. K., M. J. Cooper, and P. A. Wilson (2005), Upper Albian–lower Cenomanian calcareous nannofossil data from ODP Leg 171B, *IGBP PAGES/WDCA Contrib. Ser. 2005-036*, ftp://ftp.ncdc.noaa.gov/pub/data/paleo/contributions_by_author/watkins2005/, World Data Cent. for Paleoclimatol., Boulder, Colo.

Williams, J. R., and T. J. Bralower (1995), Nannofossil assemblages, fine fraction stable isotopes, and the paleoceanography of the Valanginian-Barremian (Early Cretaceous) North Sea Basin, *Paleoceanography*, *10*, 815–839.

Wilson, P. A., and R. D. Norris (2001), Warm tropical ocean surface and global anoxia during the mid-Cretaceous period, *Nature*, *412*, 425–428.

Wilson, P. A., R. D. Norris, and M. J. Cooper (2002), Testing the Cretaceous greenhouse hypothesis using "glassy" foraminiferal calcite from the core of the Turonian tropics on Demerara Rise, *Geology*, *30*, 607–610.

Winter, A., R. W. Jordan, and P. H. Roth (1994), Biogeography of living coccolithophores in ocean waters, in *Coccolithophores*, edited by A. Winter and W. G. Siesser, pp. 161–179, Cambridge Univ. Press, New York.

Ziveri, P., H. Stoll, I. Probert, C. Klaas, M. Geisen, G. Ganssen, and J. Young (2003), Stable isotope 'vital effects' in coccolith calcite, *Earth Planet. Sci. Lett.*, *210*, 137–149.

M. J. Cooper and P. A. Wilson, Southampton Oceanography Centre, School of Ocean and Earth Science, European Way, Southampton SO14 3ZH, UK.

D. K. Watkins, Department of Geosciences, University of Nebraska, Lincoln, NE, 68588-0340, USA. (dwatkins1@unl.edu)